Molecular Crystals and Liquid Crystals Science and Technology. Section A. Molecular Crystals and Liquid Crystals
Publication details, including instructions for authors and subscription information:
http://www.tandfonline.com/loi/gmcl19

Electro-Optical Waveguide-Spectroscopy and -Microscopy

E. Aust [a], W. Hickel [b], H. Knobloch [a], H. Orendi [a] & W. Knoll [a]
[a] Frontier Research Program, The Institute of Chemical and Physical Research (RIKEN), 2-1 Hirosawa, Wako, Saitama, 351-01, Japan
[b] Hoechst AG, Angewandte Physik, 6230 Frankfurt/Main 80, Germany

Version of record first published: 24 Sep 2006.

To cite this article: E. Aust , W. Hickel , H. Knobloch , H. Orendi & W. Knoll (1993): Electro-Optical Waveguide-Spectroscopy and -Microscopy, Molecular Crystals and Liquid Crystals Science and Technology. Section A. Molecular Crystals and Liquid Crystals, 227:1, 49-59

To link to this article: http://dx.doi.org/10.1080/10587259308030960

Mol. Cryst. Liq. Cryst. 1993, Vol. 227, pp. 49–59
Reprints available directly from the publisher
Photocopying permitted by license only

Printed in the United States of America

ELECTRO-OPTICAL WAVEGUIDE-SPECTROSCOPY AND -MICROSCOPY

E. AUST, W. HICKEL*, H. KNOBLOCH, H. ORENDI, W. KNOLL
Frontier Research Program, The Institute of Chemical and Physical Research (RIKEN), 2-1 Hirosawa, Wako, Saitama 351-01, Japan

* Hoechst AG, Angewandte Physik, 6230 Frankfurt/Main 80, Germany

Abstract This paper deals with the application of some recently developed evanescent wave-optical techniques for the characterization of electro-optically active macromolecular systems. In particular, guided optical wave-spectroscopies and -microscopies are used to determine the linear and nonlinear optical properties.

INTRODUCTION

The possible use of polymeric components for integrated optics devices requires firstly improved functionalized materials with optimized linear and nonlinear optical properties. But there is also a strong need for experimental methods that allow for a better control of various preparation steps as well as for a detailed analysis of the sample performance and the underlying structure(order)/property relation. After an introduction into the theory of the electro-optical (EO)-effect investigated by guided optical wave-spectroscopy and -microscopy, we report here on two different aspects of these studies. The first concerns the analysis of the EO-response of multilayered planar waveguide structures prepared by the Langmuir-Blodgett-Kuhn (LBK) technique[1]. The second example is the application of a recently developed novel microscopic technique[2] using guided optical waves. This electro-optic waveguide microscopy (EOWM) is capable of visualizing lateral fluctuations of the optical

anisotropy induced by the non-uniform chromophore poling process as well as of the resulting heterogeneitis of the EO-coefficients[3].

ELECTRO-OPTIC EFFECT INVESTIGATED BY WAVEGUIDE-SPECTROSCOPY

In order to introduce optical waveguide-spectroscopy we first explain the evanescent waves of surface plasmons[4]. Plasmon surface polaritons (PSPs)[5] acts as an oscillator that can be driven by the electromagnetic wave impinging upon the interface of the nearly free electron gas in the thin (~ 45 nm) Au-film evaporated onto the base of the prism shown in Fig. 1.a (top) in a so called Kretschmann configuration[6]. This resonance phenomenon can be clearly seen in the (attenuated total reflection) ATR-scan (see bottom of Fig. 1.a). Above Θ_c, the critical angle, where the reflectivity R reaches unity, the total internal reflection shows a relatively narrow dip indicating the resonant excitation of such a PSP wave at the metal - air interface.

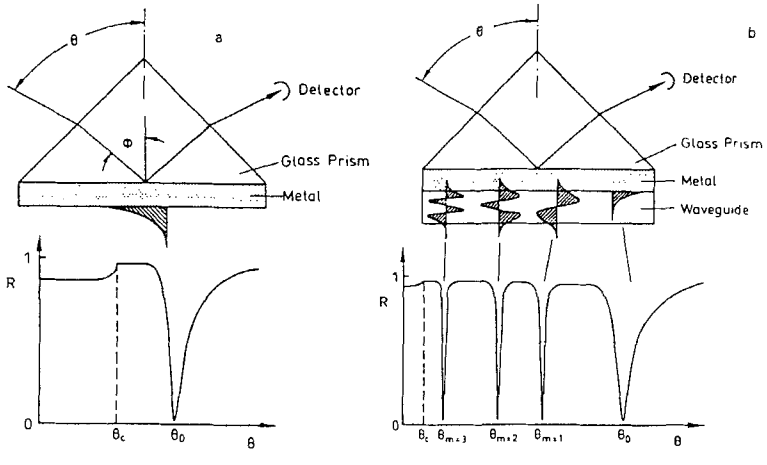

FIGURE 1 a. Resonant exitation of the plasmon surface polariton(PSP), 1 b Excitation of various guided modes

Surface plasmons as well as guided optical waves are well-defined modes that obey a known dispersion relation ω vs. k. This is schematically depicted in Fig. 2. The full curve represents the dispersion of the surface plasmons at a metal/air interface (PSP^0). The thin straight line at ω_L intersects with this dispersion curve at $k_{sp}{}^0$ and thus defines the coupling angle Θ_0. A thin dielectric coating causes a shift of the dispersion curve (PSP^1) to higer momentum (see Eq. 1) and shifts the resonance to higher

$$k_{sp}{}^1 = k_{sp}{}^0 + \Delta k_{sp} \qquad (1)$$

angle Θ_1. From this shift one can calculate the optical thickness of the coating[7].

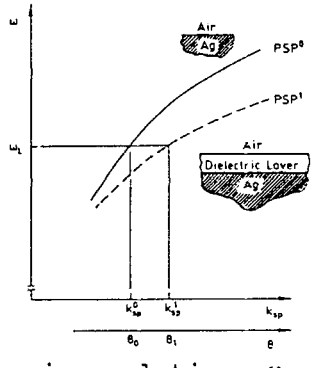

FIGURE 2. Dispersion relation, ω vs. k_{sp}.

If the thickness of the coating is further increased, a new type of non-radiative mode, guided optical waves, can be observed. This is schematically illustrated in Fig. 1b, upper part. Generally, these modes can be exited if the light travelling inside such a thin slab configuration is totally reflected at the boundaries to the surrounding media and fulfills the well-known mode equation[8]

$$kd + \beta_0 + \beta_1 = m\pi \qquad (2)$$

with k being the wavevector of the mode of order m, d the thickness of the waveguide structure and $2\beta_i = r_i''/r_i'$ with $r_i = r_i' + ir_i''$ the complex reflection coefficient at the interface between waveguide and metal, and waveguide and air, respectivly. Our configuration is somewhat special

in that this geometry ensures that guided light is constantly coupled out again through the prism so that the propagation length L is also reduced to a few μm necessary for the microscopic use of these modes. What makes guided optical waves a particularly valuable diagnostic tool is the fact that they can be excited with both TM- and TE-light, i.e. with p- and s-polarized photons.

For electro-optical layers it becomes necessary to apply a voltage in order to induce the Pockels-effect, which leads to a change of the refractive index n. A typical experimental arrangement for EO-spectroscopy or EO-microscopy is schematically sketched in Fig. 3. The change

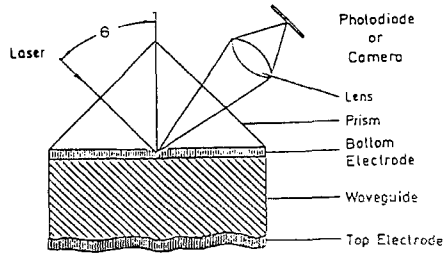

FIGURE 3. Schematic of the EO-microscopy set up or EO-spectroscopy set up (Photodiode instead of Camera) in the Kretschmann-configuration.

of n shifts the coupling angle of the different waveguide-modes according to the dispersion relation mentioned above. Fig. 4.a shows the shape of a mode, both in the absence of, and in the presence of, an applied E-field. Fig 4.b. shows the resulting differential reflectivity mode ΔR, which look's like the first derivative of the reflectivity mode R. As is well known, some materials not only exhibit a refractive index change Δn, but also display a piezo-electric effect Δd. As a result of this piezoelectric effect, the thickness changes when a voltage is applied to the electrodes. Since every mode is a solution to the Fresnel theory, it is also possible to determine both

values d and n, by measuring more modes than the number of free parameters

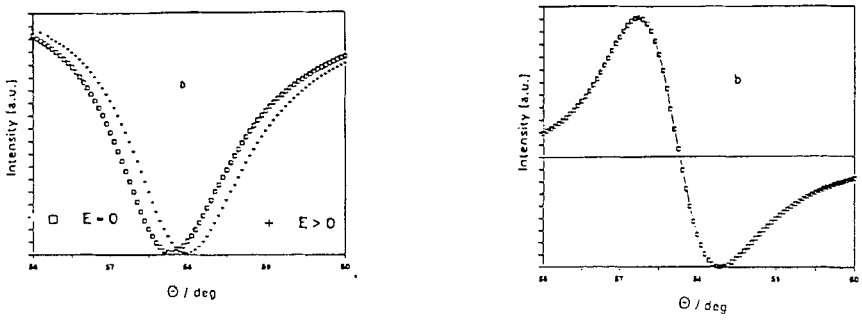

FIGURE 4a. Mode-shift by applying an E-field, 4b measured differential reflectivity mode ΔR.

Even for the EO-constant, and the piezoelectric-constant, it is possible to distinguish these parameters with the total differential shown in Eq. 3.

$$\Delta R = \delta R/\delta n_{o,e} * \Delta n_{o,e} + \delta R/\delta d * \Delta d \quad (3)$$

The different polarisation of light (TM- or TE-light) allows now to check the quality of the calculations.

ELECTRO-OPTICS WITH LBK-MULTILAYER ASSEMBLIES

Because every mode of a guided wave represents a different E- field distribution in the light-conducting material (see Fig 1.b lower part), the EO-response is strongly dependent on this shape. The full control of the layer architecture of planar waveguides prepared by the LBK-technique allows for a detailed analysis of the EO-response of $\chi^{(2)}$-active, multilayered samples. Our system was built-up from a noncentrosymmetric A-B alternate layer sample (50 layers each) with A being the NLO active dye (see Fig 5.a) and B being the counter layers, composed of inert trimethylsilanecellulose molecules sandwiched between 210 spacer layers on each side of material C (see Fig. 5.b).

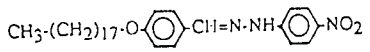

a

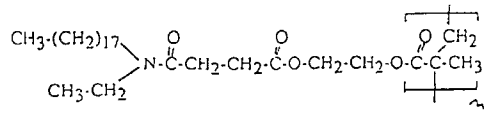

b

FIGURE 5. Materials used for the LBK-multilayer assemblies

The mode pattern of this multilayer waveguide between gold electrodes is shown in Fig 6.a for s-, and in Fig 6.b for p-polarized light of λ = 633 nm, respectively. Their Fresnel-analysis (see full lines in Figs. 6.a and b) yield the thickness and anisotropic refractive index data.

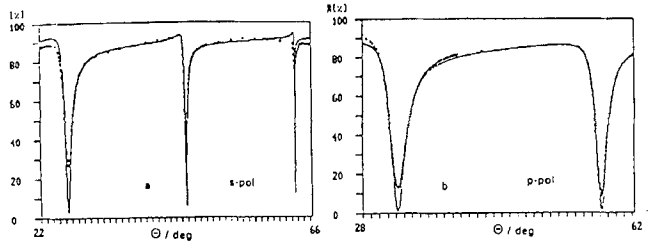

FIGURE 6. Mode pattern of the multilayered waveguide for s-polarized (a) and p-polarized light (b)

If an AC voltage of U_{eff} = 10.6 V is applied to the 0.8 μm thick film a Pockels-response is observed by lock-in amplifier detection as it is shown in Fig. 7.a for s-, and in Fig. 7.b for p-polarized light. Clearly, the different modes show a very different EO-response. This is interpreted as being caused by the different (optical) field intensity distributions found within the waveguide structure for the various modes. The calculated field for the m=0, m=1 for s-, and m=2 and m=3 for the p-polarized light are given in Fig. 8.a (s-pol) and 8.b (p-pol), respectively. One can see, that the m=1 mode (s-pol) or m=3 (p-pol) has a node in the middle of the waveguide(where th

A-B layer is located) and hence exhibits only the weak EO-response seen in Fig. 7.

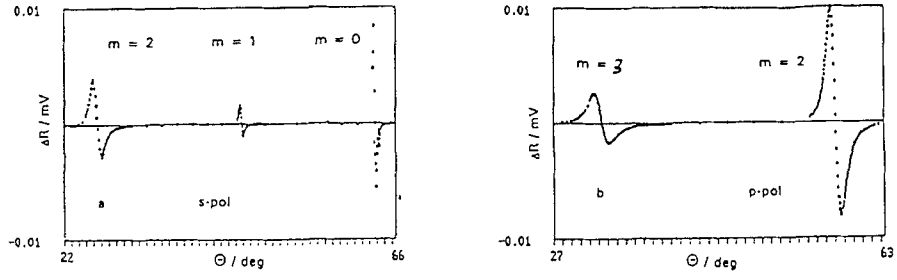

Figure 7. Pockels-response ΔR of the s-polarized mode pattern (a), and of the p-polarized mode pattern (b)

The m = 0 mode for s-pol and m = 2 mode for p-pol on the other hand, has its field maximum in the EO-active layer. The quantitative evaluation of the $\chi(2)_{13}$ coefficients, show for all three modes similar values: $\chi(2)_{13}$ = 13.5 pm/V (12.3 -14.3 pm/V), and for the $\chi(2)_{33}$ coefficient, the two modes show similar values: $\chi(2)_{33}$ = 21.3 pm/V

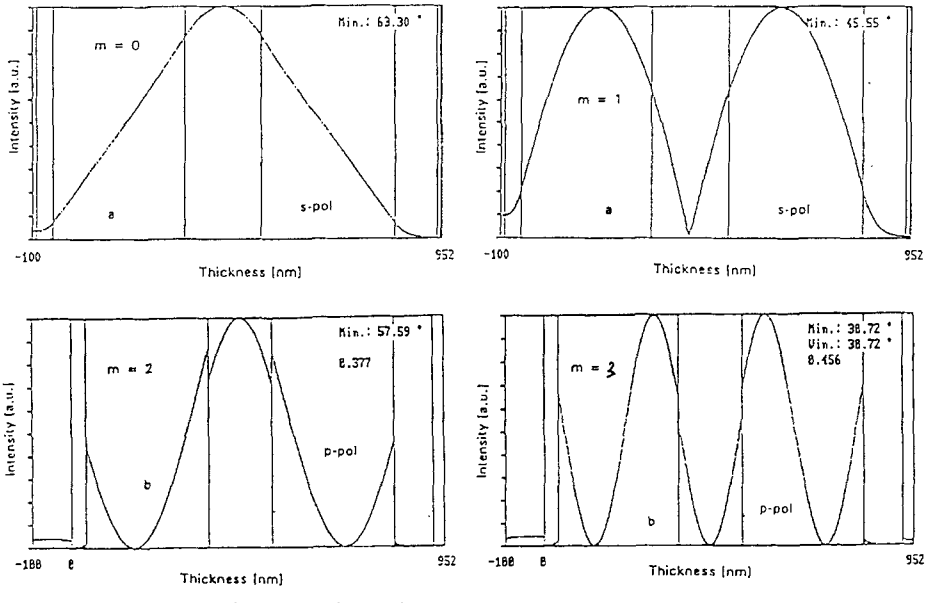

FIGURE 8. E-field distribution for the m=0 mode and m=1 mode for s-polarized light (a), anf for m=2 mode and m=3 mode for p-polarized light (b).

ELECTRO-OPTICAL WAVEGUIDE MICROSCOPY

Recently we introduced optical waveguide microscopy[2] as a novel analytical tool well-suited to characterize planar waveguide structures. The schematic set-up which is very similar to a surface plasmon microscope[4] is given in Fig. 3. The laser is resonantly coupled by means of the prism to the optical modes that can be guided in the polymer film between the two metal electrodes. If the waveguide is laterally heterogeneous in thickness and/or refractive index (as it is highly exaggerated in Fig. 3) the local waveguide resonances can be monitored by imaging the structure on a TV camera with the help of a lens that Fourier-backtransforms the scattered and out-coupled guided light. A series of such OWM-pictures is given in Fig. 9. With increasing angle of incidence Θ the local resonance clearly seen as the dark region in the pictures moves across the frame following the increasing waveguide thickness. This solid polyelectrolyte film with an isotropic index of refraction of n=1.63 had a thickness variation across the imaged area of 570*420mm^2 ranging from d=325 nm to d=348 nm. The obtainable resolutions where shown to be Δd=1nm for the thickness and Δl=5μm for the lateral dimensions. This latter value is only obtainable for such a highly lossy configuration (see Fig. 3) which reduces the propagation length of the modes correspondingly.

Now, if we are concerned with nonlinear optically functionalized materials, e.g., a chromophore-doped polymer, the requirement of the non-centro-symmetry for the chromophore orientation distribution for electro-optic or frequency doubling (SHG) devices may introduce other additional heterogeneities that limit the device performance: if the poling process typically used to orient the functional units results in a laterally heterogeneous distribution function we have to deal with fluctuations of the (anisotropic) index of refraction as well as of the

nonlinear response, e.g., a spatial variation of the EO-coefficients r_{33} and r_{13}. This is demonstrated in Fig. 10.

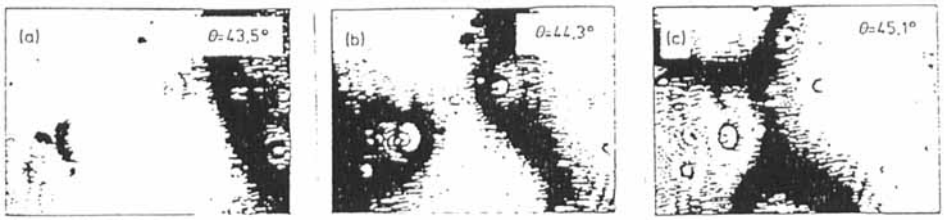

FIGURE 9 (a) - (c) series of OWM pictures taken at different angles of incidence.

Each data point is obtained by recording the reflected intensity from small local areas (typically 20*20μm^2) in pictures like the ones presented in Fig. 9. For this purpose an image analysis computer routine sets little frames at various positions in the stored pictures and calculates the pixel gray value histograms from these frames. Their average gray value is then plotted in Fig. 10 as a function of time.

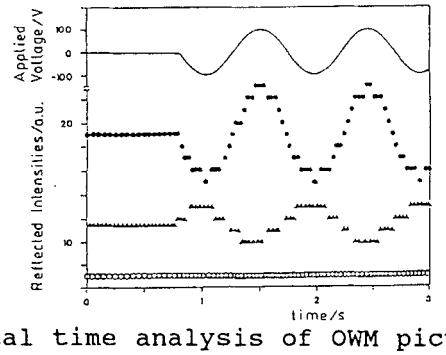

FIGURE 10 Real time analysis of OWM pictures like the ones presented in Fig. 9. Shown are the mean reflected intensities as obtained from the pixel gray value histograms calculated from different areas on the waveguide structure under the influence of an applied voltage (full curve).

Prior to the application of any voltage the different levels of the reflected intensities from different areas

(see the 3 different symbols in Fig. 10) correspond to the static optical heterogeneity of the sample which is a combination of the lateral fluctuations of the geometrical thickness and of the optical anisotropy of the refractive index caused by an inhomogeneous poling process.

Once a (slowly) alternating voltage is applied between the two electrodes, the monitored local reflectivities are also modulated by the Pockels effect. The possible time resolution is in our case ca 60 Hz given by the frame transfer time of our CCD-camera but could be as high as 10 kHz given recent developments in high speed CCD-cameras[9]. These changes can be recorded very sensitively. Note, e.g., that the example given in Fig. 10 was obtained with a Disperse Red 1 doped poly(methylmethacrylate) waveguide which was poled and then aged for 1 week. The residual chromophore orientation and its heterogeneity, therfore, was very weak. The sign and the amplitude of the AC-response for a given fixed angle of incidence, Θ_0, depends on the static angular position of the local resonances. If the monitored area has its resonance (in the absence of an E-field) at a higher angle then the EO-effect induced shift of the (local) mode to smaller angles will cause a decrease of the reflected intensity (full circles in Fig. 10). If the local mode is resonant at smaller angles the same shift causes an intensity increase (full triangles in Fig. 10).

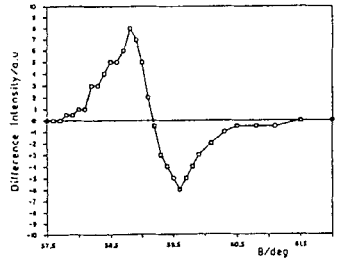

FIGURE 11. Angular dependence of the peak-to-peak amplitude taken from modulation plots like the ones presented in Fig. 10 but for a single local area.

Right in the resonance the response can be negligable (open circles).

If one monitors the amplitude of modulation for one chosen area as a function of the angle of incidence one obtains the differentiated mode spectrum $\delta R/\delta E$ (see Fig. 11) known from EO-waveguide experiments with lock-in detection[10,11]. In our case, however, the corresponding analysis of these data in terms of the EO-coefficients is not smeared by the above mentioned heterogeneities but rather reflects the true local EO-response of the poled polymer.

ACKNOWLEDGEMENTS

Helpfull discussions with S. Herminghaus, D. Morichere, J.D. Swalen, T. Wada, H. Sasabe and Y. Levy are gratefully acknowleged. We thank P. Gross and V. Macho for their help with the software. This work was financially supported by the Volkswagen Stiftung (I/66 109).

REFERENCES

1. H: Kuhn. D. Möbius and H. Bücher in Physical Methods of Chemistry edited by A. Weissberger and B.W. Rossiter (Wiley, New York, 1972)Part III B. Chap. VII
2. W. Hickel and W. Knoll, Appl. Phys. Lett. 57, 1286, (1990)
3. E.F. Aust and W. Knoll, Appl. Phy. Lett. 00, 000 (1992)
4. W. Knoll, MRS Bulletin XVI (7), 29 (1991)
5. E. Burstein, W.P. Chen, Y.J. Chen and A.Hartstein, J. Vac. Sci. Technol. 11, (1974) p. 1004
6. E. Kretschmann, Opt. Commun. 6, (1972) p. 185
7. J.G. Gordon, J.D. Swalen, Opt. Commun. 22, 374 (1977)
8. P.K. Tien, Rev. Mod. Phys. 49, 361 (1961)
9. G. Matsumodo, presented at the 1st Int. Conf. on Intelligent Materials, Osio, Japan, (1992)
10. M. Dumont, Y. Levy and D. Morichere, in Organic Molecules for Nonlinear Optics and Photonics, edited by J. Messier (NATO ASI Series, Kluwer Academic Publisher)
11. R.H. Page, M.C. Jurich, B. Reck, A. Sen, R.Twieg J.D. Swalen, G.C. Bjorklund and C.G. Willson, J. Opt. Soc. Am. B7, 1239 (1990)